Article:
Diaz-Pinto, A, Ravikumar, N, Attar, R et al. (2022) Predicting myocardial infarction through retinal scans and minimal personal information. Nature Machine Intelligence, 4. pp. 55-61. ISSN: 2522-5839

https://doi.org/10.1038/s42256-021-00427-7

Predicting Myocardial Infarction through Retinal Scans and Minimal Personal Information

Andres Diaz-Pinto[a,b,*], Nishant Ravikumar[a,b], Rahman Attar[a,b], Avan Suinesiaputra[a,b], Yitian Zhao[g], Eylem Levelt[b,d], Erica Dall'Armellina[b,d], Marco Lorenzi[h], Qingyu Chen[i], Tiarnan D. L. Keenan[j], Elvira Agrón[j], Emily Y. Chew[j], Zhiyong Lu[i], Chris P. Gale[b,c,d], Richard P. Gale[e,f], Sven Plein[b,d], Alejandro F. Frangi[a,b,k,l,m,*]

[a] *Centre for Computational Imaging and Simulation Technologies in Biomedicine, School of Computing, University of Leeds, Leeds, UK.*
[b] *Leeds Institute for Cardiovascular and Metabolic Medicine, School of Medicine, University of Leeds, Leeds, UK.*
[c] *Leeds Institute for Data Analytics, University of Leeds, Leeds UK.*
[d] *Department of Cardiology, Leeds Teaching Hospitals NHS Trust, Leeds, UK.*
[e] *Department of Ophthalmology, York Teaching Hospital NHS Foundation Trust, York, UK*
[f] *Department of Health Sciences, University of York, York, UK*
[g] *Cixi Institute of Biomedical Engineering, Ningbo Institute of Materials, Technology and Engineering, Chinese Academy of Sciences, Ningbo, China*
[h] *Université Côte d'Azur, Inria Sophia Antipolis, Epione Project-Team, France*
[i] *National Center for Biotechnology Information, National Library of Medicine, NIH, Bethesda, MD, USA*
[j] *Division of Epidemiology and Clinical Applications, National Eye Institute, NIH, Bethesda, MD, USA*
[k] *Department of Cardiovascular Sciences, KU Leuven, Leuven, Belgium*
[l] *Department of Electrical Engineering, KU Leuven, Leuven, Belgium*
[m] *Alan Turing Institute, London, UK*

Abstract

In ophthalmologic practice, retinal images are routinely obtained to diagnose and monitor primary eye diseases and systemic conditions affecting the eye, such as diabetic retinopathy. Recent studies have shown that biomarkers on retinal images, e.g. retinal blood vessels density or tortuosity, are associated with cardiac function and may identify patients at risk of coronary artery disease. In this work, we investigate the use of retinal images alongside relevant patient metadata, to estimate left ventricular mass (LVM) and left ventricular end-diastolic volume (LVEDV), and subsequently, predict incident myocardial infarction. We trained a multi-channel variational autoencoder (mcVAE) and a deep regressor model to estimate LVM (4.4 (-32.30, 41.1) g) and LVEDV (3.02 (-53.45, 59.49) ml) and predict risk of myocardial infarction (AUC=0.80$\pm$ 0.02, Sensitivity=0.74 $\pm$ 0.02, Specificity=0.71 $\pm$ 0.03) using just the retinal images and demographic data. Our results indicate that one could identify patients at high risk of future myocardial infarction from retinal imaging available in every optician and eye clinic.

Keywords: UK Biobank, AREDS, Retinal Images, Cardiac MRI, Multi-Channel VAE

Introduction

Cardiovascular diseases (CVD) represent a major cause of death and socio-economic burden globally. In 2015 alone, there were ∼18 million CVD-related deaths worldwide [1]. Identification and timely treatment of CVD risk factors is a key strategy for reducing CVD prevalence in populations and for risk modulation in individuals. Conventionally, CVD risk is estimated using demographic/clinical parameters such as age, sex, ethnicity, smoking status, family history, history of hyperlipidaemia, diabetes mellitus or hypertension [2]. Imaging tests such as coronary computed tomography, echocardiography and cardiovascular magnetic resonance (CMR) help further stratify patient risk, by assess-

*Corresponding authors
Email addresses: andres.diaz-pinto@kcl.ac.uk (Andres Diaz-Pinto), a.frangi@leeds.ac.uk (Alejandro F. Frangi)

ing coronary calcium burden, myocardial scar burden, ischaemia, cardiac chamber size and function.

Cardiovascular imaging is usually performed in secondary care and is relatively expensive, limiting its availability in under-developed and developing countries. An alternative approach to risk stratification is to use the information available from non-cardiac investigations. Retinal microvascular abnormalities, such as generalised arteriolar narrowing, focal arteriolar narrowing, and arterio-venous nicking have shown strong associations with systemic, and cardiovascular disease, such as diabetes mellitus, hypertension and coronary artery disease [3, 4]. Retinal images (including details of principal blood vessels) are now routinely acquired in optometric and ophthalmologic practice and are relatively inexpensive. Retinal images could, therefore, be a potential cost-effective screening tool for cardiovascular disease. Beyond risk prediction, retinal images have also been associated with cardiovascular phenotypes such as left ventricular dimensions and mass [3, 4]. Poplin *et al.* showed for the first time that retinal images allowed prediction of cardiovascular risk factors such as age, gender, smoking status, systolic blood pressure and major adverse cardiac events [5], driven by anatomical features such as the optic disc or retinal blood vessels. This highlighted the potential for using retinal images to assess risk of cardiovascular diseases.

We explore new ways to extend this line of research, by learning a combined representation of retinal images and cardiac magnetic resonance (CMR) images, to assess cardiac function and predict myocardial infarction events. This is supported by the work of Cheung *et al.* [6], who highlighted the adverse effects of blood pressure and cardiac dysfunction on retinal microvasculature. Similarly, Tapp *et al.* [7] established associations between retinal vessel morphology and cardiovascular disease risk factors and/or CVD outcomes using a multilevel linear regressor. This study assessed the relationships between retinal vessel morphometry, blood pressure, and arterial stiffness index, furthering our understanding of preclinical disease processes and the interplay between microvascular and macrovascular diseases. Using retinal fundus images, Gargeya *et al.* [8] and Qummar *et al.* [9] used deep learning to detect diabetes, and classify different grades of diabetic retinopathy, respectively. These studies demonstrate the efficacy of deep learning techniques to quantify and stratify cardiovascular disease risk factors, given retinal images. Other studies such as Pickhardt *et al.* [10] utilised whole-body CT scans and deep learning to predict future adverse cardiovascular events, further supporting the hypothesis that alternate image modalities, covering multiple organs, help assess cardiovascular health and predict CVD risk.

As markers of cardiovascular diseases are often manifested in the retina, images of this organ could identify future cardiovascular events such as left ventricular hypertrophy or myocardial infarction. This work proposes a novel method that estimates cardiac indices and predicts incident myocardial infarction based on retinal images and demographic data from the UKB. For myocardial infarction, we only considered incidents that occurred after the retinal image was taken. Our approach uses a multi-channel variational autoencoder trained on two channels of information: retinal and CMR images from the same subject. This method combines features extracted from both imaging modalities in a common latent space, allowing us to use that latent space to subsequently estimate relevant quantities from just one channel of information (i.e. retinal images) and demographic data. Applied to clinical practice, estimation of cardiac indices from retinal images could guide patients at risk of CVDs to cardiologists following a routine ophthalmic check or directly predicting myocardial infarction based on the retinal and minimal demographic data.

Experiments and Results

In this study, we jointly trained a multi-channel VAE (mcVAE) and a deep regressor network on CMR, retinal images and demographic data from participants in the UKB cohort. As the first experiment, we used manual and automatic delineations of the CMR images as ground truth to estimate LVM and LVEDV from retinal images. These manually delineated images were analysed by a team of eight experts using the commercially available **cvi42** post-processing software (Circle Cardiovascular Imaging Inc., Calgary, Canada) [30]. On the other hand, the automatic delineations were obtained from the method proposed by Attar *et al.* [31]. The main motivation for this set of experiments is to perform a fair comparison between our system and the state-of-the-art methods. It is worth mentioning that all methods published in the literature that used the UKB cohort, are trained using the aforementioned manual delineations. Results of this experiment are presented in Bland-

Altman and Pearson's correlation plots (See Figure 1(a)).

Figure 1(a) denotes the correlation between the LVM ($r = 0.65$) and LVEDV ($r = 0.45$) values estimated using our approach, and the ones manually computed from the CMR images using cvi42 software. The results obtained from this experiment support the clinical findings published years ago by clinical researchers in [32, 3, 4]. They found that retinal images could be potentially used to quantify parameters in the heart.

Besides the Bland-Altman and correlation plots, we also compared our proposed method against the state-of-the-art methods for cardiac quantification using CMR images (Bai et al. [33]), including the Siemens Inline VF system (See Extended Data Table 4). The Siemens Inline VF system was the first fully automatic left ventricular analysis tools commercially available [34]. D13 and E11C versions have been currently used as a baseline for comparison against manual delineation [30].

Bland-Altman plots and Pearson's correlation were computed for the participants with automatic annotations for LVM and LVEDV (see Figure 1(b)).

Figure 1(b) shows a significant correlation between the LVM and LVEDV estimated by the proposed method and parameters computed from Attar's algorithm. We also found that using more images to train our method positively impacts the obtained error (See Extended Data Table 4 Exp 2B).

As it was shown, our approach can estimate LVM and LVEDV from the retinal images and demographic data. In addition to this, it can also be used to improve the prediction of future MI events. To demonstrate this, we compare MI prediction in two settings: 1) using only demographic data, and 2) using LVM/LVEDV (predicted using our approach) plus demographic data. To do that, we performed 10-fold cross-validation on subjects not previously used for training and a logistic regression model (See Figure 2).

Figure 2 (right) shows a significant increase in the area under the ROC curve when using LVM/LVEDV plus demographics to predict MI.

Besides predicting myocardial infarction, we also compared the estimated LVM/LVEDV values between the MI cases and no-MI cases using a t-test. Here, the null hypothesis is that the LVM/LVEDV values come from the same distribution, while the alternative hypothesis is that these values come from different distributions. We consider that the obtained results are different if the p-value is less than 0.05. According to experimental results, a p-value of $1.43e^{-57}$ and $2.32e^{-52}$ were obtained for LVM and LVEDV correspondingly, meaning we rejected the null hypothesis and LVM/LVEDV values for MI no-MI cases come from different distributions.

Additional experiments evaluating the Frechet Inception Distance (FID) [35] score for reconstructed CMR images (Supplementary Figure 2) and the impact of the retinal image size (Supplementary Figure 4), training set size (Supplementary Figure 5), and different demographic variables (Supplementary Figure 7) to the proposed algorithm are presented in the Supplementary Material Section 5

External Validation

Finally, external validation using the optimal model identified from the preceding experiments was carried out. This validation was conducted on the AREDS dataset using retinal images and the demographic data presented in Extended Data Table 1. As previously mentioned, this dataset is composed of 3,010 participants in total. From these participants, there are 180 participants with MI events and 2,830 with no-MI events.

We used the mcVAE trained on all the 5,663 retinal images available of size 128×128px. In the AREDS dataset, the demographic data available differed from that in the UKB. We trained our method for the available metadata in the AREDS. This means variables such as systolic blood pressure, diastolic blood pressure, smoking status, alcohol consumption status, body mass index, age, and gender were used for the external validation. The demographic variable "alcohol consumption" was converted to a continuous variable — in terms of gm/day consumed. The remaining variables are consistent between datasets in the way they are coded.

As the AREDS dataset was initially used because of the detailed information of AMD, we performed three analyses discarding different levels of AMD to show the impact AMD has on MI prediction. The obtained results can be seen in Figure 3 and Table 1.

Discussion

The present study demonstrates that retinal images and demographic data could be of great value

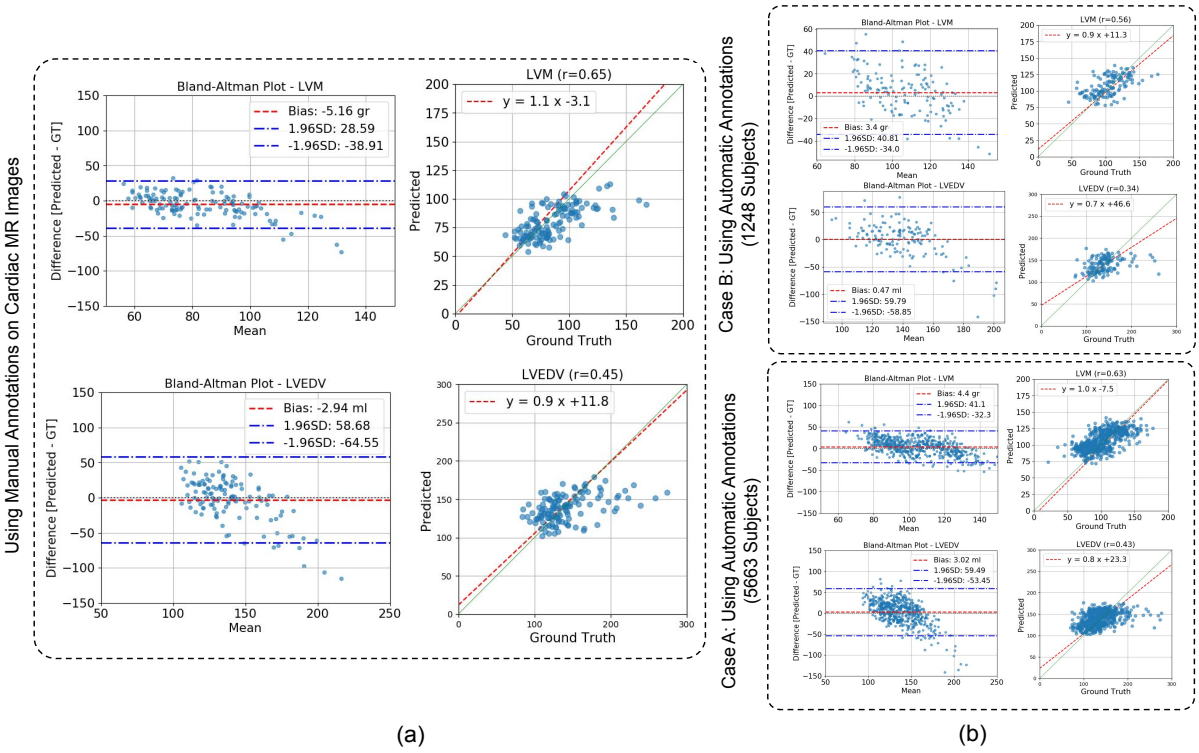

Figure 1: **Estimation of LVM and LVEDV using manual and automatic annotations:** (a) Bland-Altman and correlation plots for estimated LVM and LVEDV using manual annotations on CMR images. (b) Bland-Altman and correlation plots for estimated LVM and LVEDV using automatic annotations computed from Attar *et al.* [31] method. In Case A, we used all the available subjects to train and test our method. *The solid line represents the logistic regression, and the dotted line represents the line of identity.*

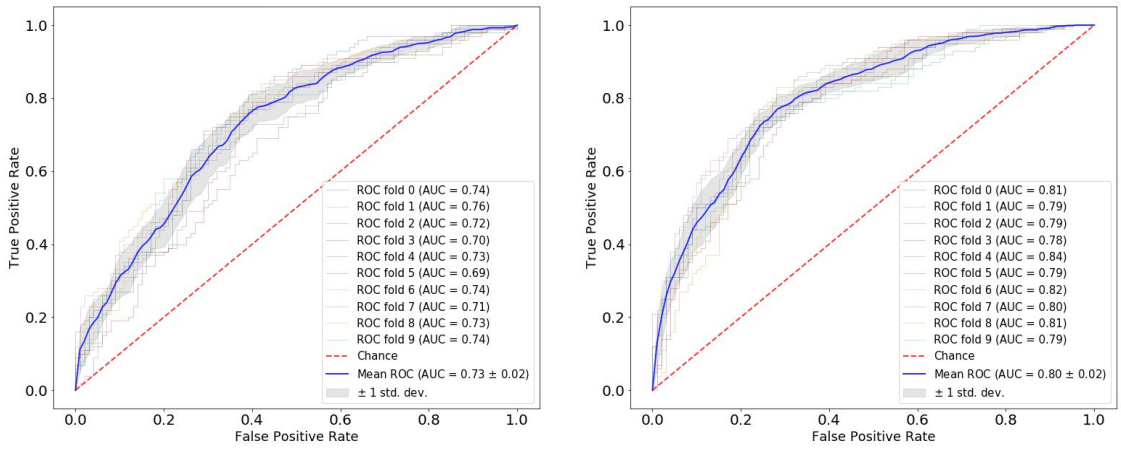

Figure 2: **Cross-validation results for MI prediction:** ROC curves obtained for MI prediction using only demographic data. Accuracy: 0.66 ± 0.03, Sensitivity: 0.7 ± 0.04, Specificity: 0.64 ± 0.03, Precision: 0.64 ± 0.03, and F1 Score: 0.66 ± 0.03 (left). ROC curves obtained for MI prediction using LVM, LVEDV (derived from the proposed pipeline) and demographic data. Accuracy: 0.74 ± 0.03, Sensitivity: 0.74 ± 0.02, Specificity: 0.71 ± 0.03, Precision: 0.73 ± 0.05, and F1 Score: 0.74 ± 0.03. (right).

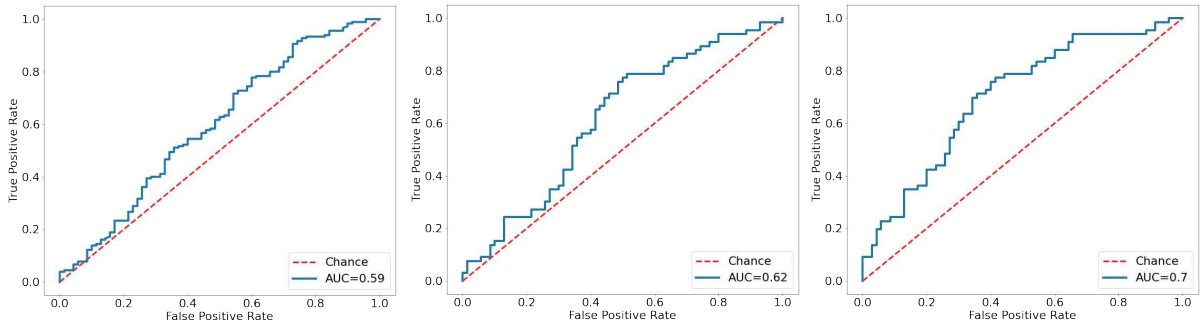

Figure 3: **ROC curves obtained from the external validation using AREDS dataset:** (a) ROC curve obtained considering all the AMD cases, (b) ROC curve obtained after discarding AMD cases with labels 2 and 3, and (c) ROC curve obtained after excluding all AMD cases (labels 1, 2 and 3).

Table 1: **Obtained results from the external validation using AREDS dataset:** Accuracy, Sensitivity, Specificity, Precision and F1 Score were computed to show the impact of AMD on the MI prediction.

	Accuracy	**Sensitivity**	**Specificity**	**Precision**	**F1 Score**
Considering all AMD cases	0.59	0.70	0.49	0.49	0.57
Discarding AMD labels 2 & 3	0.62	0.70	0.54	0.54	0.61
Excluding all AMD cases	0.68	0.70	0.67	0.67	0.68

to estimate cardiac indices such as the LV mass (LVM) and LV end-diastolic volume (LVEDV) by jointly learning a latent space retinal and CMR images. To the best of our knowledge, no previous works use a multi-modal approach with retinal and CMR to learn a joint latent space and subsequently estimate cardiac indices using just retinal and demographic data. Our results follow previous research demonstrating strong associations between biomarkers in the retina and the heart [3, 4, 32], similar to what has been shown in a recent study where, cardiovascular risk factors such as age, gender, blood pressure were quantified using only retinal images [5].

Using the proposed method to estimate LVM and LVEDV, we can assess patients at risk of future MI or risk of similar adverse cardiovascular events at routine ophthalmic visits. This would enable patient referral for further examination. Besides this, estimated LVM/LVEDV could also be used to provide insights into pathological cardiac remodelling or hypertension at no extra cost. This means, if an ophthalmologist keeps a record of those indices for their patient over time, they can refer patients for further assessment to cardiologists, if a significant increase in the LVM or LVEDV is detected. The ophthalmologist could be bypassed with automated risk detection if patients consented to share their data on the cloud.

Figure 1 shows that our trained model is less powerful at estimating higher LVM and LVEDV. Two main factors are involved here: (1) The proportion of subjects with elevated LVM/LVEDV available for training (with retinal images) is limited, and (2) Retinal images do not contain "all" the information to assess cardiac function.

We chose to predict LVM and LVEDV as an intermediate step rather than directly predicting future MI events because: (1) this ensures that the developed approach is flexible in its clinical application, as it could be used not just to predict MI, but to assess LV function in general; (2) using LVM and LVEDV enhances the explainability of predictions, as evidenced by the analysis of the logistic regression coefficients presented in the supplementary material.

In the external validation analyses, we presented detailed data on the relative performance of the algorithm to predict incident MI, according to the presence and severity of AMD in the retinal images. The performance was highest in the absence of AMD and appeared to decrease with the inclusion of individuals with AMD of gradually increasing severity. In its most severe form, neovas-

cular AMD, the disease can cause extensive fibrosis, haemorrhage, and exudation across much of the macula; this is likely to obliterate the relevant signals employed by the algorithm for predicting incident MI. Even in less severe forms, such as early and intermediate AMD, substantial alterations to macular anatomy are observed, including drusen and pigmentary abnormalities [36], which may partially degrade or interfere with the relevant signals. We might assume that the most important signals from the retinal images, for MI prediction, are encoded in the retinal vessels [5]. In this case, even early and intermediate AMD are accompanied by substantial changes in the retinal vasculature's quantitative and morphological features [37]. Overall, the presence of retinal disease such as AMD, particularly in its more severe forms, presumably interferes with the ability of the algorithm to infer characteristics of the systemic circulation from the retinal circulation.

The AUC scores obtained using our approach for UKBB and AREDS populations has to be considered in the context of a second referral setting at an optician/eye clinic and not a primary cardiology clinic. The sensitivity, specificity and precision/positive predictive value (PPV) of our approach at predicting future MI events from retinal images in - (a) the UKBB population were 0.74, 0.72 and 0.68, respectively, when just Age and Gender were considered as additional demographic variables (representative of the information available in an optician/eye clinic), as highlighted in Supplementary Figure 7; and (b) the AREDS population, after excluding all AMD cases, was 0.70, 0.67, and 0.67 respectively. Established cardiovascular disease risk assessment models (e.g. Framingham Risk Score (FRS), Systemic Coronary Risk Evaluation (SCORE), Pooled Cohort Equation (PCE) etc.) [38, 39, 40, 41] used previously to screen populations for atherosclerotic cardiovascular disease are comparable to our approach in discriminatory capacity, while requiring several additional demographic variables and clinical measurements not readily available at an optician/eye clinic. For instance, in [39] the authors compare FRS, PCE and SCORE in the multi-ethnic study of atherosclerosis, each achieving an AUC of 0.717, 0.737 and 0.721, respectively, and corresponding sensitivity and specificity of 0.7-0.8 and 0.5-0.6, respectively. Similarly, in [38] multiple cardiovascular risk assessment models were compared in their sensitivity, specificity and PPV on the Diabetes and Cardiovascular Risk Evaluation: Targets and Essential Data for Commitment of Treatment study. This study revealed that FRS and PCE's sensitivity, specificity, and PPV ranged from 0.56-0.78, 0.60-0.78 and 0.12-0.24, respectively, when considering a 10% risk threshold. While the performance of our approach in this study cannot be directly compared to the risk assessment models evaluated in either of the studies above, they provide context to the results obtained on both UKBB and AREDS populations, highlighting its potential for use as a second referral tool at an eye clinic/optician. However, it is important to note that this is a proof of concept study with limitations in study design (detailed in the supplementary material for brevity), predominantly the limited availability of the multi-modal data required for such analyses.

Conclusion

This study presents a system that estimates cardiac indices such as LVM and LVEDV and predicts future MI events using inexpensive and easy to obtain retinal photographs and demographic data. We used 5,663 subjects from the UKB imaging study with end-diastolic cardiac MR, retinal images and demographic data to train and test our method. We used this system to predict MI in subjects that have retinal images and were not used during the training process. We found that using cardiac indices and demographic data together, yields significant improvements in predicting MI events compared with using only demographic data. Finally, we performed an independent replication study of our method on the AREDS dataset. Although a drop in performance was observed, the discrimination capacity of our approach remained comparable to established CVD risk assessment models reported previously. This highlights the potential for our approach to be employed as a second referral tool in eye clinics/opticians, to identify patients at risk of future MI events. Future work will explore genetic data to improve the discriminatory capacity of the proposed approach and explainable artificial intelligence techniques to identify the dominant retinal phenotypes that help assess CVD risk. This will help facilitate fine-grained stratification of CVD risk in patients, which will be a crucial step towards delivering personalised medicine.

Image datasets and demographic data

This study used CMR images (end-diastolic short-axis view), retinal images, and demographic data from the UKB cohort (under access application #11350) were used to train and validate the proposed method. When this method was developed, 39,705 participants underwent CMR imaging using a clinical wide bore 1.5 Tesla MRI system (MAGNETOM Aera, Syngo Platform VD13A, Siemens Healthcare, Erlangen, Germany) [11], and 84,760 participants underwent retinal imaging using a Topcon 3D OCT 1000 Mark 2 (45° field-of-view, centred to include both optic disc and macula) [12]. Only those participants with CMR, retinal images, and demographic data were selected to train our proposed method, totalling 11,383 participants.

From 11,383 participants, 676 participants were excluded due to a history of conditions known to affect LV mass such as diabetes (336 subjects), previous myocardial infarction (293 subjects), cardiomyopathy (14 subjects) or frequent strenuous exercise routines (33 subjects).

After excluding participants with the conditions above, a deep learning method for quality assessment (QA) [13] was used to obtain the retinal images of sufficient quality, as per certain pre-specified criteria. This QA method utilises the public dataset called EyePACS [14], a well-known dataset presented in the Kaggle platform for automatic diabetic retinopathy detection, to train and validate its performance. Following QA, 5,663 participants were identified to have good quality retinal images. We followed the RECORD statement for reporting observational data, and a STROBE flow diagram showing the exclusion criteria is presented in Figure 4. Subsequent preprocessing steps for retinal and CMR images (i.e. ROI detection [15]) are presented in Supplementary Material Section 1.

Regarding the demographic data, a combination of variables derived from the patient's history and blood samples such as sex, age, gender, HbA1c, systolic and diastolic blood pressure, smoking habit, alcohol consumption, glucose and body mass index were also used as input to train and test the proposed method. Although we excluded participants with diabetes, we retain HbA1c as multiple studies have shown positive correlation of HbA1c with cardiovascular mortality even in subjects without a history of diabetes [16, 17, 18]. Additionally, in [19] the authors showed a strong association between HbA1c and LV mass. They found that a 1% rise in HbA1c level was associated with a 3.0 g increase in LV mass in elderly subjects. All these variables are summarised in Extended Data Table 3.

Besides demographic data, we also utilised LVEDV and LVM extracted directly from the CMR images. These cardiac indices were computed from the manual delineations [20] generated using **cvi42** post-processing software, and segmentations generated automatically using the method proposed by Attar *et al.* [21]. More details about how these values were used are outlined in the Experiments and Results sections.

Age-Related Eye Disease Study (AREDS) database

The Age-Related Eye Disease Study (AREDS) was a multicenter prospective study of the clinical course of age-related macular degeneration (AMD) and age-related cataract, as well as a phase III randomised controlled trial designed to assess the effects of nutritional supplements on AMD and cataract progression [22, 23]. Institutional review board approval was obtained at each clinical site and written informed consent for the research was obtained from all study participants. The research was conducted under the Declaration of Helsinki. Additional information on AREDS and associated demographic data is included in the Supplementary Material Section 2

Code Availability Statement

All algorithms used in this study were developed using libraries and scripts in PyTorch. Source code is publicly available at [42].

Data Availability

UKB images are reproduced with the kind permission of UK Biobank ©. All UKB images and demographic data are available, with restrictions, from UK Biobank. Researchers who use the UKB dataset must first complete the UK Biobank online Access Management System (AMS) application form. More information for accessing the UKB dataset can be found in this link: `https://www.ukbiobank.ac.uk/enable-your-research/apply-for-access`
The AREDS data set (NCT00000145) is available in the dbGAP repository, `https://www.ncbi.nlm.nih.gov/projects/gap/cgi-bin/study.cgi?study_id=phs000001.v3.p1`

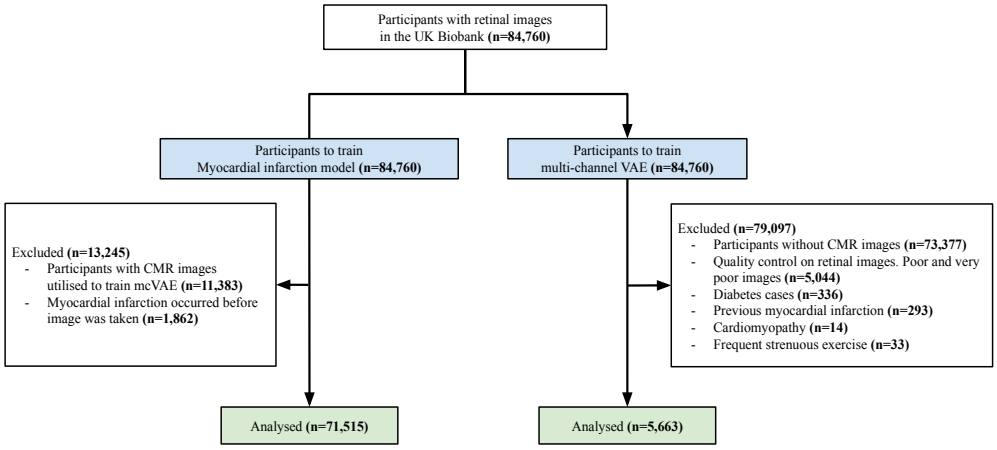

Figure 4: **STROBE flow diagram for excluded participants:** Criteria for excluding participants in this study.

Methods

Our method is based on the multi-channel variational autoencoder (mcVAE) [24] and a deep regression network (`github.com/cistib/MI_prediction_retina_mcVAE`) (ResNet50). For the mcVAE, we designed two pairs of encoder/decoders to train the network, in which each pair is trained on one of the two data channels (retinal and CMR images), with a shared latent space. The full diagram of the proposed method is presented in Figure 5. Details of the encoders and the decoders are described in Extended Data Table 3.

Antelmi *et al.* [24] highlighted that using a sparse version of the mcVAE ensures the evidence lower bound generally reaches the maximum value at convergence when the number of latent dimensions coincides with the true one used to generate the data. Consequently, we used the sparse version of the mcVAE. We trained a sparse latent space z for both channels of information. A detailed explanation of how mcVAE works and the difference between this and a vanilla VAE [25, 26, 27, 28] is provided in Supplementary Material Section 3

Once the mcVAE was trained, we used the learned latent space to train the deep regressor (ResNet50). To do that, we used CMR images reconstructed from the retinal images plus the demographic data (Stage II in Figure 5).

Prediction of Incident Myocardial Infarction

We evaluate the ability of the proposed approach to estimate LVM and LVEDV from the retinal images and demographic data. As an additional experiment, we predict myocardial infarction (MI) utilising logistic regression in two settings: 1) using the demographic data alone; and 2) using LVM/LVEDV estimated from the retinal images and the demographic data, and subsequently, combined with the latter for predicting MI. Logistic regression eased interpretability, allowing us to compare the weights/coefficients of the variables towards the final prediction (See Figure 3). We extract the cases with MI events from the participants not used to train the system to make this comparison. This means, 73,477 participants out of a total 84,760 participants with retinal images. Of the 73,477, 2,954 subjects have previous MI. However, we only consider the cases where MI occurred after the retinal images were taken, which results in 992 MI cases and 70,523 no-MI cases.

We are dealing with imbalanced data. Hence, we randomly resampled the normal cases to the same number of MI cases (992). Previous studies [29] have highlighted that resampling the majority class is a robust solution when having hundreds of cases in the minority class. Once the majority class was resampled, we performed 10-fold cross-validation using logistic regression to predict MI in the scenarios described previously (i.e. using only demographic and using demographic plus LVM/LVEDV).

Acknowledgements

AFF is supported by the Royal Academy of Engineering Chair in Emerging Technologies Scheme (CiET1819\19), the MedIAN Network (EP/N026993/1) funded by the Engineering and Physical Sciences Research Council (EPSRC). This

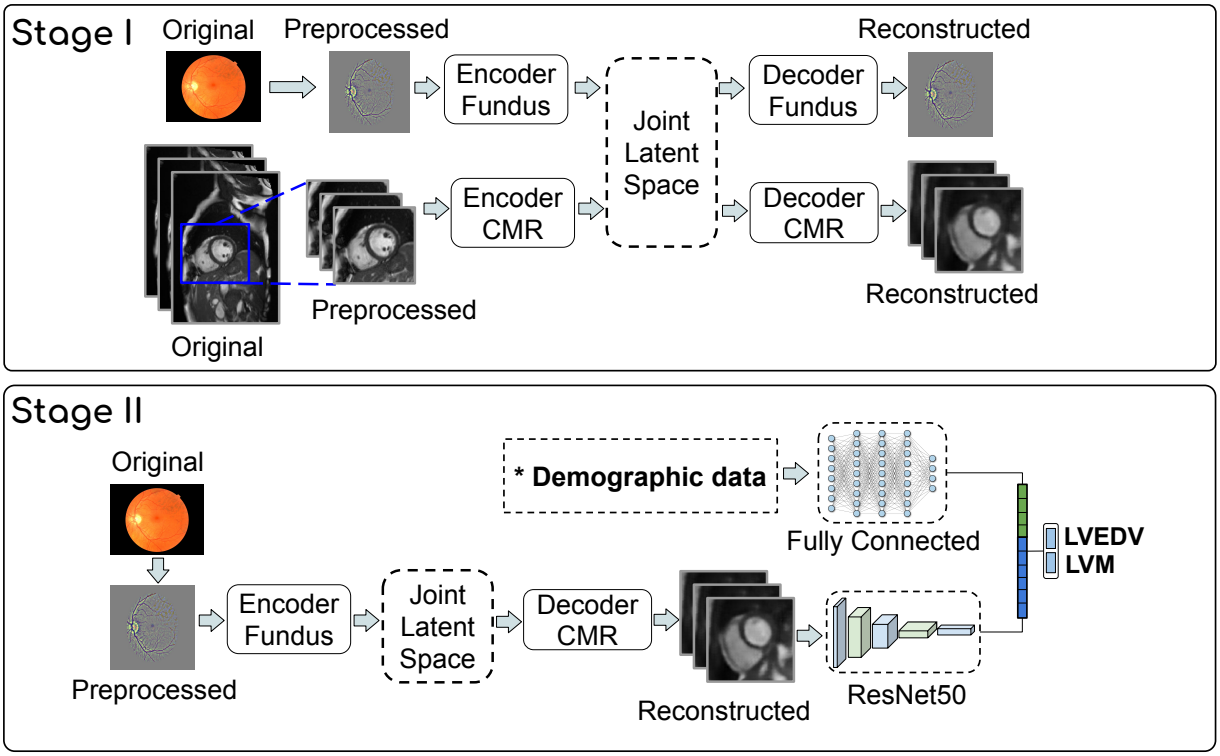

*** Details of the demographic data**

Characteristics	Age (years)	Female (%)	BMI (kg/m^2)	DBP (mmHg)	SBP (mmHg)	HbA1c (mmol/mol)	Glucose (mmol/L)	Cholesterol (mmol/L)	Smoker (%)	Drinker (%)
Training set	58.72 (7.43)	48.39	26.47 (4.38)	79.42 (15.51)	132.24 (26.55)	31.83 (11.45)	4.20 (2.26)	5.20 (2.10)	5.77	2.15
Test set	58.90 (7.46)	52.10	26.71 (4.36)	80.85 (15.53)	134.82 (25.10)	31.30 (12.34)	4.20 (2.18)	5.25 (2.11)	5.21	2.18

BMI: Body Mass Index, DBP: Diastolic Blood Pressure, SBP: Systolic Blood Pressure

Figure 5: **Overview of the proposed method:** This system comprises two main components, a multi-channel VAE and a deep regressor network. During Stage I, a joint latent space is created with two channels: Retinal and cardiac MR. Then, during Stage II a deep regressor is trained on the reconstructed CMR plus demographic data to estimate LVM and LVEDV. **Demographic data:** Summary of the subjects metadata used in this study to train (5097 participants) and test (566 participants) the proposed method. All continuous values are reported in mean and standard deviation (in parenthesis) while categorical data are reported in percentage (%).These images were reproduced with the kind permission of UKB©.

work was also supported by the Intramural Research Program of National Library of Medicine and National Eye Institute, National Institutes of Health. Additionally, this research was supported by the European Union's Horizon 2020 InSilc (777119) and EPSRC TUSCA (EP/V04799X/1) programmes. Erica Dall'Armellina acknowledges funding from the BHF grant FS/13/71/30378.

Author Contributions

A.D.-P. designed and executed all experiments, conducted all subsequent statistical analyses, and drafted the manuscript. N.R. helped design the experiments, helped with the writing, data interpretation and made substantial revisions and edits of the draft manuscript. R.A. helped design the experiments, contributed to the data analysis and data cleaning. A.S. and Y.Z. contributed to the data analysis. E.L., E.D.A., C.P.G, R.P.G., S.P. contributed to the analysis of retinal and cardiac MR images and shaped the medical contribution of this work. M.L. contributed to the design and implementation of the mcVAE. Q.C., T.D.L.K., E.A., E.Y.C., Z.L. contributed to the external validation of the proposed method. A.F.F. helped design the experiments and contributed to the writing. All authors contributed to the manuscript.

Competing Interests

The authors declare that they have no competing financial interests.

References

[1] G. A. Roth, C. Johnson, A. Abajobir, F. Abd-Allah, S. F. Abera, G. Abyu, M. Ahmed, B. Aksut, and et al., "Global, Regional, and National Burden of Cardiovascular Diseases for 10 Causes, 1990 to 2015," *Journal of the American College of Cardiology*, vol. 70, no. 1, pp. 1 – 25, 2017.

[2] R. B. D'Agostino, R. S. Vasan, M. J. Pencina, P. A. Wolf, M. Cobain, J. M. Massaro, and W. B. Kannel, "General Cardiovascular Risk Profile for Use in Primary Care," *Circulation*, vol. 117, no. 6, pp. 743–753, 2008.

[3] T. Y. Wong, R. Klein, B. E. K. Klein, J. M. Tielsch, L. Hubbard, and F. J. Nieto, "Retinal microvascular abnormalities and their relationship with hypertension, cardiovascular disease, and mortality.," *Survey of ophthalmology*, vol. 46 1, pp. 59–80, 2001.

[4] B. R. McClintic, J. I. McClintic, J. D. Bisognano, and R. C. Block, "The relationship between retinal microvascular abnormalities and coronary heart disease: a review," *The American journal of medicine*, vol. 123, no. 4, pp. 374–e1, 2010.

[5] R. Poplin, A. V. Varadarajan, K. Blumer, Y. Liu, M. V. McConnell, G. S. Corrado, L. Peng, and D. R. Webster, "Predicting Cardiovascular Risk Factors from Retinal Fundus Photographs using Deep Learning," *Nat Biomed Eng*, vol. 2, pp. 158 – 164, 2018.

[6] C. Cheung, W. Tay, P. Mitchell, J. Wang, W. Hsu, M. Lee, Q. Lau, A. Zhu, R. Klein, S. Saw, and T. Wong, "Quantitative and qualitative retinal microvascular characteristics and blood pressure," *Journal of Hypertension*, vol. 27, pp. 1380 – 1391, 2011.

[7] R. J. Tapp, C. G. Owen, S. A. Barman, R. A. Welikala, P. J. Foster, P. H. Whincup, D. P. Strachan, A. R. Rudnicka, and null null, "Associations of Retinal Microvascular Diameters and Tortuosity With Blood Pressure and Arterial Stiffness," *Hypertension*, vol. 74, no. 6, pp. 1383–1390, 2019.

[8] R. Gargeya and T. Leng, "Automated Identification of Diabetic Retinopathy Using Deep Learning," *Ophthalmology*, vol. 124, no. 7, pp. 962 – 969, 2017.

[9] S. Qummar, F. G. Khan, S. Shah, A. Khan, S. Shamshirband, Z. U. Rehman, I. Ahmed Khan, and W. Jadoon, "A Deep Learning Ensemble Approach for Diabetic Retinopathy Detection," *IEEE Access*, vol. 7, pp. 150530–150539, 2019.

[10] P. J. Pickhardt, P. M. Graffy, R. Zea, S. J. Lee, J. Liu, V. Sandfort, and R. M. Summers, "Automated CT biomarkers for opportunistic prediction of future cardiovascular events and mortality in an asymptomatic screening population: a retrospective cohort study," *The Lancet Digital Health*, vol. 2, no. 4, pp. e192 – e200, 2020.

[11] S. E. Petersen, P. M. Matthews, J. M. Francis, M. D. Robson, F. Zemrak, R. Boubertakh, A. A. Young, S. Hudson, P. Weale, S. Garratt, R. Collins, S. Piechnik, and S. Neubauer, "UK Biobank's cardiovascular magnetic resonance protocol," *Journal of Cardiovascular Magnetic Resonance*, vol. 18, pp. 1 – 7, 2015.

[12] T. J. MacGillivray, J. R. Cameron, Q. Zhang, A. El-Medany, C. Mulholland, Z. Sheng, B. Dhillon, F. N. Doubal, P. J. Foster, E. Trucco, C. Sudlow, U. B. Eye, and V. Consortium, "Suitability of UK Biobank Retinal Images for Automatic Analysis of Morphometric Properties of the Vasculature," *PLOS ONE*, vol. 10, pp. 1–10, 05 2015.

[13] H. Fu, B. Wang, J. Shen, S. Cui, Y. Xu, J. Liu, and L. Shao, "Evaluation of Retinal Image Quality Assessment Networks in Different Color-Spaces," in *Medical Image Computing and Computer Assisted Intervention – MICCAI 2019*, (Cham), pp. 48–56, Springer International Publishing, 2019.

[14] Kaggle, "Kaggle diabetic retinopathy competition." `https://www.kaggle.com/c/diabetic-retinopathy-detection/data`, 2015. Accessed: 2020-01-19.

[15] Q. Zheng, H. Delingette, N. Duchateau, and N. Ayache, "3-D Consistent and Robust Segmentation of Cardiac Images by Deep Learning With Spatial Propagation," *IEEE Transactions on Medical Imaging*, vol. 37, pp. 2137–2148, Sep. 2018.

[16] K.-T. Khaw, N. Wareham, S. Bingham, R. Luben, A. Welch, and N. Day, "Association of Hemoglobin A1c with Cardiovascular Disease and Mortality in Adults: The European Prospective Investigation into Cancer in Norfolk," *Annals of Internal Medicine*, vol. 141, no. 6, pp. 413–420, 2004. PMID: 15381514.

[17] E. Levitan, S. Liu, M. Stampfer, N. Cook, K. Rexrode, P. Ridker, J. Buring, and J. Manson, "Hba1c measured in stored erythrocytes and mortality rate among middle-aged and older women," *Diabetologia*, vol. 51, no. 2, pp. 267–275, 2008.

[18] H. C. Gerstein, K. Swedberg, J. Carlsson, J. J. McMurray, E. L. Michelson, B. Olofsson, M. A. Pfeffer, and S. Yusuf, "The hemoglobin A1c level as a progressive risk factor for cardiovascular death, hospitalization for heart failure, or death in patients with chronic heart failure: an analysis of the Candesartan in Heart failure: Assessment of Reduction in Mortality and Morbidity (CHARM) program," *Archives of internal medicine*, vol. 168, no. 15, pp. 1699–1704, 2008.

[19] H. Skali, A. Shah, D. K. Gupta, S. Cheng, B. Claggett, J. Liu, N. Bello, D. Aguilar, O. Vardeny, K. Matsushita, *et al.*, "Cardiac structure and function across the glycemic spectrum in elderly men and women free of prevalent heart disease: the atherosclerosis risk in the community study," *Circulation: Heart Failure*, vol. 8, no. 3, pp. 448–454, 2015.

[20] S. E. Petersen, N. Aung, M. M. Sanghvi, F. Zemrak, K. Fung, J. Miguel Paiva, J. M. Francis, M. Y. Khanji, E. Lukaschuk, A. Lee, *et al.*, "Reference ranges for cardiac structure and function in cardiovascular magnetic resonance (cmr) imaging in caucasians from the uk biobank population cohort," *Journal of Cardiovascular Magnetic Resonance*, vol. 19, no. 1, 2017.

[21] R. Attar, M. Pereañez, C. Bowles, S. K. Piechnik, S. Neubauer, S. E. Petersen, and A. F. Frangi, "3D Cardiac Shape Prediction with Deep Neural Networks: Simultaneous Use of Images and Patient Metadata," in *Medical Image Computing and Computer Assisted Intervention – MICCAI 2019*, (Cham), pp. 586–594, Springer International Publishing, 2019.

[22] T. A.-R. E. D. S. R. Group, "The Age-Related Eye Disease Study (AREDS): Design Implications AREDS

Report No. 1," *Controlled Clinical Trials*, vol. 20, no. 6, pp. 573–600, 1999.

[23] A.-R. E. D. S. R. Group *et al.*, "The Age-Related Eye Disease Study system for classifying age-related macular degeneration from stereoscopic color fundus photographs: the Age-Related Eye Disease Study Report Number 6," *American journal of ophthalmology*, vol. 132, no. 5, pp. 668–681, 2001.

[24] L. Antelmi, N. Ayache, P. Robert, and M. Lorenzi, "Sparse Multi-Channel Variational Autoencoder for the Joint Analysis of Heterogeneous Data," in *Proceedings of the 36th International Conference on Machine Learning*, vol. 97, pp. 302–311, PMLR, 09–15 Jun 2019.

[25] D. P. Kingma and M. Welling, "Auto-Encoding Variational Bayes," *Proceedings 2nd International Conference on Learning Representations (ICLR)*, 2014.

[26] D. J. Rezende, S. Mohamed, and D. Wierstra, "Stochastic Backpropagation and Approximate Inference in Deep Generative Models," *arXiv preprint arXiv:1401.4082*, 2014.

[27] H. Hotelling, "Relations between two sets of variates," *Biometrika*, vol. 28, no. 3/4, pp. 321–377, 1936.

[28] S. Haufe, F. Meinecke, K. Görgen, S. Dähne, J.-D. Haynes, B. Blankertz, and F. Bießmann, "On the interpretation of weight vectors of linear models in multivariate neuroimaging," *NeuroImage*, vol. 87, pp. 96 – 110, 2014.

[29] J. M. Johnson and T. M. Khoshgoftaar, "Survey on deep learning with class imbalance," *Journal of Big Data*, vol. 6, no. 1, p. 27, 2019.

[30] A. Suinesiaputra, M. M. Sanghvi, N. Aung, J. M. Paiva, F. Zemrak, K. Fung, E. Lukaschuk, A. M. Lee, V. Carapella, Y. J. Kim, *et al.*, "Fully-automated left ventricular mass and volume MRI analysis in the UK Biobank population cohort: evaluation of initial results," *The international journal of cardiovascular imaging*, vol. 34, no. 2, pp. 281–291, 2018.

[31] R. Attar, M. Pereañez, A. Gooya, X. Albà, L. Zhang, M. H. de Vila, A. M. Lee, N. Aung, E. Lukaschuk, M. M. Sanghvi, K. Fung, J. M. Paiva, S. K. Piechnik, S. Neubauer, S. E. Petersen, and A. F. Frangi, "Quantitative CMR population imaging on 20,000 subjects of the UK biobank imaging study: LV/RV quantification pipeline and its evaluation," *Medical Image Analysis*, vol. 56, pp. 26 – 42, 2019.

[32] N. Keith, "Some different types of essential hypertension: their course and prognosis," *American Journal of the Medical Sciences*, vol. 268, pp. 336–345, 1974.

[33] W. Bai, M. Sinclair, G. Tarroni, O. Oktay, M. Rajchl, G. Vaillant, A. M. Lee, N. Aung, E. Lukaschuk, M. M. Sanghvi, *et al.*, "Automated cardiovascular magnetic resonance image analysis with fully convolutional networks," *Journal of Cardiovascular Magnetic Resonance*, vol. 20, no. 1, p. 65, 2018.

[34] K. Lin, J. D. Collins, D. M. Lloyd-Jones, M.-P. Jolly, D. Li, M. Markl, and J. C. Carr, ""automated assessment of left ventricular function and mass using heart deformation analysis:: Initial experience in 160 older adults"," *Academic Radiology*, vol. 23, no. 3, pp. 321 – 325, 2016.

[35] M. Heusel, H. Ramsauer, T. Unterthiner, B. Nessler, and S. Hochreiter, "GANs Trained by a Two Time-Scale Update Rule Converge to a Local Nash Equilibrium," in *Advances in Neural Information Processing Systems*, vol. 30, Curran Associates, Inc., 2017.

[36] F. L. Ferris, C. Wilkinson, A. Bird, U. Chakravarthy, E. Chew, K. Csaky, and S. R. Sadda, "Clinical classification of age-related macular degeneration," *Ophthalmology*, vol. 120, no. 4, pp. 844–851, 2013.

[37] M. Trinh, M. Kalloniatis, and L. Nivison-Smith, "Vascular Changes in Intermediate Age-Related Macular Degeneration Quantified Using Optical Coherence Tomography Angiography," *Translational Vision Science & Technology*, vol. 8, pp. 20–20, 08 2019.

[38] T. B. Grammer, A. Dressel, I. Gergei, M. E. Kleber, U. Laufs, H. Scharnagl, U. Nixdorff, J. Klotsche, L. Pieper, D. Pittrow, *et al.*, "Cardiovascular risk algorithms in primary care: Results from the detect study," *Scientific reports*, vol. 9, no. 1, pp. 1–12, 2019.

[39] W. T. Qureshi, E. D. Michos, P. Flueckiger, M. Blaha, V. Sandfort, D. M. Herrington, G. Burke, and J. Yeboah, "Impact of replacing the pooled cohort equation with other cardiovascular disease risk scores on atherosclerotic cardiovascular disease risk assessment (from the multi-ethnic study of atherosclerosis [mesa])," *The American journal of cardiology*, vol. 118, no. 5, pp. 691–696, 2016.

[40] C. Wallisch, G. Heinze, C. Rinner, G. Mundigler, W. C. Winkelmayer, and D. Dunkler, "External validation of two framingham cardiovascular risk equations and the pooled cohort equations: a nationwide registry analysis," *International journal of cardiology*, vol. 283, pp. 165–170, 2019.

[41] C. Wallisch, G. Heinze, C. Rinner, G. Mundigler, W. C. Winkelmayer, and D. Dunkler, "Re-estimation improved the performance of two framingham cardiovascular risk equations and the pooled cohort equations: a nationwide registry analysis," *Scientific reports*, vol. 10, no. 1, pp. 1–11, 2020.

[42] A. D. Pinto, "Predicting myocardial infarction through retinal scans and minimal personal information," *https://doi.org/10.5281/zenodo.5716142*, 2021.